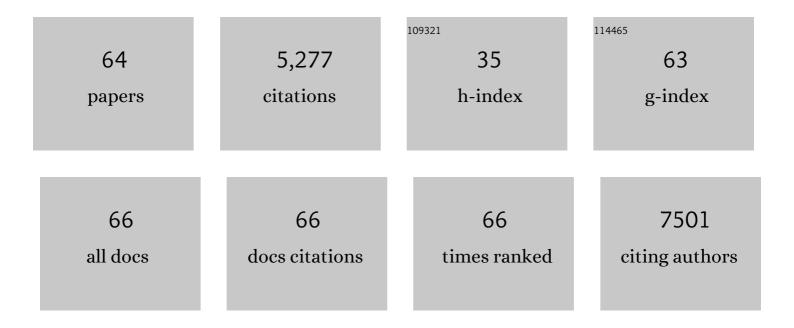
Xi-Lin Wu

List of Publications by Year in descending order

Source: https://exaly.com/author-pdf/2421658/publications.pdf Version: 2024-02-01



#	Article	IF	CITATIONS
1	Biomass-Derived Sponge-like Carbonaceous Hydrogels and Aerogels for Supercapacitors. ACS Nano, 2013, 7, 3589-3597.	14.6	557
2	Synthesis of Magnetite/Graphene Oxide Composite and Application for Cobalt(II) Removal. Journal of Physical Chemistry C, 2011, 115, 25234-25240.	3.1	386
3	One-step hydrothermal synthesis of N-doped TiO ₂ /C nanocomposites with high visible light photocatalytic activity. Nanoscale, 2012, 4, 576-584.	5.6	332
4	One-Pot Synthesis of Water-Swellable Mg–Al Layered Double Hydroxides and Graphene Oxide Nanocomposites for Efficient Removal of As(V) from Aqueous Solutions. ACS Applied Materials & Interfaces, 2013, 5, 3304-3311.	8.0	310
5	Water-dispersible magnetite-graphene-LDH composites for efficient arsenate removal. Journal of Materials Chemistry, 2011, 21, 17353.	6.7	240
6	Spherical α-Ni(OH)2 nanoarchitecture grown on graphene as advanced electrochemical pseudocapacitor materials. Chemical Communications, 2012, 48, 2773.	4.1	223
7	Membrane fouling in a membrane bioreactor: High filtration resistance of gel layer and its underlying mechanism. Water Research, 2016, 102, 82-89.	11.3	209
8	Oxygen deficient ZnO _{1â^'x} nanosheets with high visible light photocatalytic activity. Nanoscale, 2015, 7, 7216-7223.	5.6	190
9	Coexistence of adsorption and coagulation processes of both arsenate and NOM from contaminated groundwater by nanocrystallined Mg/Al layered double hydroxides. Water Research, 2013, 47, 4159-4168.	11.3	150
10	Stable Organic–Inorganic Hybrid of Polyaniline/α-Zirconium Phosphate for Efficient Removal of Organic Pollutants in Water Environment. ACS Applied Materials & Interfaces, 2012, 4, 2686-2692.	8.0	144
11	Molecular Engineering toward Pyrrolic Nâ€Rich Mâ€N ₄ (M = Cr, Mn, Fe, Co, Cu) Singleâ€Atom Sites for Enhanced Heterogeneous Fentonâ€Like Reaction. Advanced Functional Materials, 2021, 31, 2007877.	14.9	139
12	Carbonaceous hydrogels and aerogels for supercapacitors. Journal of Materials Chemistry A, 2014, 2, 4852-4864.	10.3	137
13	Effect of calcium ions on fouling properties of alginate solution and its mechanisms. Journal of Membrane Science, 2017, 525, 320-329.	8.2	131
14	Efficient degradation and mineralization of antibiotics via heterogeneous activation of peroxymonosulfate by using graphene supported single-atom Cu catalyst. Chemical Engineering Journal, 2020, 394, 124904.	12.7	117
15	Terbium-based infinite coordination polymer hollow microspheres: preparation and white-light emission. Journal of Materials Chemistry, 2011, 21, 16574.	6.7	111
16	Effects of molecular weight distribution of soluble microbial products (SMPs) on membrane fouling in a membrane bioreactor (MBR): Novel mechanistic insights. Chemosphere, 2020, 248, 126013.	8.2	97
17	Enhanced visible-light-driven photocatalysis from WS ₂ quantum dots coupled to BiOCl nanosheets: synergistic effect and mechanism insight. Catalysis Science and Technology, 2018, 8, 201-209.	4.1	95
18	New insights into bisphenols removal by nitrogen-rich nanocarbons: Synergistic effect between adsorption and oxidative degradation. Journal of Hazardous Materials, 2018, 345, 123-130.	12.4	93

XI-LIN WU

#	Article	IF	CITATIONS
19	Facile synthesis of Fe3O4-graphene@mesoporous SiO2 nanocomposites for efficient removal of Methylene Blue. Applied Surface Science, 2016, 378, 80-86.	6.1	88
20	Green-assembly of three-dimensional porous graphene hydrogels for efficient removal of organic dyes. Journal of Colloid and Interface Science, 2016, 484, 254-262.	9.4	80
21	Impact of solution chemistry conditions on the sorption behavior of Cu(II) on Lin'an montmorillonite. Desalination, 2011, 269, 84-91.	8.2	78
22	Quantification of interfacial interactions between a rough sludge floc and membrane surface in a membrane bioreactor. Journal of Colloid and Interface Science, 2017, 490, 710-718.	9.4	69
23	Sustainable biodegradation of phenol by immobilized Bacillus sp. SAS19 with porous carbonaceous gels as carriers. Journal of Environmental Management, 2018, 222, 185-189.	7.8	68
24	Enhanced catalytic degradation of bisphenol A by hemin-MOFs supported on boron nitride via the photo-assisted heterogeneous activation of persulfate. Separation and Purification Technology, 2019, 229, 115822.	7.9	68
25	A Universal Principle to Accurately Synthesize Atomically Dispersed Metal–N4 Sites for CO2 Electroreduction. Nano-Micro Letters, 2020, 12, 108.	27.0	65
26	An ultra-sensitive electrochemical sensor for hydrazine based on AuPd nanorod alloy nanochains. Electrochimica Acta, 2016, 195, 68-76.	5.2	64
27	Insight into the mechanisms for hexavalent chromium reduction and sulfisoxazole degradation catalyzed by graphitic carbon nitride: The Yin and Yang in the photo-assisted processes. Chemosphere, 2019, 221, 166-174.	8.2	63
28	Regulating Intrinsic Electronic Structures of Transition-Metal-Based Catalysts and the Potential Applications for Electrocatalytic Water Splitting. , 2021, 3, 752-780.		62
29	Precise regulation of pyrroleâ€type singleâ€atom Mnâ€N ₄ sites for superior pHâ€universal oxygen reduction. , 2021, 3, 856-865.		60
30	Enzyme-mimicking single-atom FeN4 sites for enhanced photo-Fenton-like reactions. Applied Catalysis B: Environmental, 2022, 310, 121327.	20.2	57
31	Bamboo-like carbon nanotubes derived from colloidal polymer nanoplates for efficient removal of bisphenol A. Journal of Materials Chemistry A, 2016, 4, 15450-15456.	10.3	55
32	Biocompatible G-Fe3O4/CA nanocomposites for the removal of Methylene Blue. Journal of Molecular Liquids, 2015, 212, 63-69.	4.9	53
33	Bimetallic AuPd nanoclusters supported on graphitic carbon nitride: One-pot synthesis and enhanced electrocatalysis for oxygen reduction and hydrogen evolution. International Journal of Hydrogen Energy, 2016, 41, 8839-8846.	7.1	45
34	Organic dye doped graphitic carbon nitride with a tailored electronic structure for enhanced photocatalytic hydrogen production. Catalysis Science and Technology, 2019, 9, 502-508.	4.1	45
35	Highly efficient removal of humic acid from aqueous solutions by Mg/Al layered double hydroxides–Fe3O4 nanocomposites. RSC Advances, 2014, 4, 21802.	3.6	43
36	Synthesis of Alumina-Modified Cigarette Soot Carbon As an Adsorbent for Efficient Arsenate Removal. Industrial & Engineering Chemistry Research, 2014, 53, 16051-16060.	3.7	40

XI-LIN WU

#	Article	IF	CITATIONS
37	Morphology and Thermal Properties of Precision Polymers: The Crystallization of Butyl Branched Polyethylene and Polyphosphoesters. Macromolecules, 2016, 49, 1321-1330.	4.8	38
38	Functionalization of carbon nanomaterials by means of phytic acid for uranium enrichment. Science of the Total Environment, 2019, 694, 133697.	8.0	36
39	Highly efficient capture of Eu(III), La(III), Nd(III), Th(IV) from aqueous solutions using g-C3N4 nanosheets. Journal of Molecular Liquids, 2018, 252, 351-361.	4.9	35
40	Stable and recyclable Fe3C@CN catalyst supported on carbon felt for efficient activation of peroxymonosulfate. Journal of Colloid and Interface Science, 2021, 599, 219-226.	9.4	34
41	Facile large scale fabrication of magnetic carbon nano-onions for efficient removal of bisphenol A. Materials Chemistry and Physics, 2017, 198, 186-192.	4.0	33
42	Iron-modulated nickel cobalt phosphide embedded in carbon to boost power density of hybrid sodium–air battery. Applied Catalysis B: Environmental, 2021, 285, 119786.	20.2	32
43	Efficient electrocatalytic water splitting by bimetallic cobalt iron boride nanoparticles with controlled electronic structure. Journal of Colloid and Interface Science, 2021, 604, 650-659.	9.4	32
44	Biomass-derived multifunctional magnetite carbon aerogel nanocomposites for recyclable sequestration of ionizable aromatic organic pollutants. Chemical Engineering Journal, 2014, 245, 210-216.	12.7	31
45	Semi-sacrificial template synthesis of single-atom Ni sites supported on hollow carbon nanospheres for efficient and stable electrochemical CO ₂ reduction. Inorganic Chemistry Frontiers, 2020, 7, 1719-1725.	6.0	31
46	Hollow-structured amorphous prussian blue decorated on graphitic carbon nitride for photo-assisted activation of peroxymonosulfate. Journal of Colloid and Interface Science, 2021, 603, 856-863.	9.4	23
47	Magnetic ZnFe ₂ O ₄ @chitosan encapsulated in graphene oxide for adsorptive removal of organic dye. RSC Advances, 2017, 7, 28145-28151.	3.6	22
48	Heteroatomic Interface Engineering of MOF-Derived Metal-Embedded P- and N-Codoped Zn Node Porous Polyhedral Carbon with Enhanced Sodium-Ion Storage. ACS Applied Energy Materials, 2020, 3, 8892-8902.	5.1	20
49	Quantitative evaluation of the interfacial interactions between a randomly rough sludge floc and membrane surface in a membrane bioreactor based on fractal geometry. Bioresource Technology, 2017, 234, 198-207.	9.6	19
50	Impact of key geochemical parameters on the highly efficient sequestration of Pb(II) and Cd(II) in water using g-C3N4 nanosheets. Journal of Molecular Liquids, 2018, 258, 40-47.	4.9	18
51	Dual active sites of the Co ₂ N and single-atom Co–N ₄ embedded in nitrogen-rich nanocarbons: a robust electrocatalyst for oxygen reduction reactions. Nanotechnology, 2020, 31, 165401.	2.6	16
52	Use of molybdenum disulfide nanosheets embellished nanoiron for effective capture of chromium (VI) ions from aqueous solution. Journal of Molecular Liquids, 2018, 259, 376-383.	4.9	14
53	Highly efficient scavenging of P(V), Cr(VI), Re(VII) anions onto g-C3N4 nanosheets from aqueous solutions as impacted via water chemistry. Journal of Molecular Liquids, 2018, 258, 275-284.	4.9	13
54	Synthesizing the Composites of Graphene Oxide-Wrapped Polyaniline Hollow Microspheres for High-Performance Supercapacitors. Science of Advanced Materials, 2013, 5, 1686-1693.	0.7	13

XI-LIN WU

#	Article	IF	CITATIONS
55	Characterization of molybdenum disulfide nanomaterial and its excellent sorption abilities for two heavy metals in aqueous media. Separation Science and Technology, 2019, 54, 847-859.	2.5	9
56	Self-templated synthesis of novel carbon nanoarchitectures for efficient electrocatalysis. Scientific Reports, 2016, 6, 28049.	3.3	7
57	Application of biochar derived from rice straw for the removal of Th(IV) from aqueous solution. Separation Science and Technology, 2018, 53, 1511-1521.	2.5	6
58	Macroscopic, theoretical simulation and spectroscopic investigation on the immobilization mechanisms of Ni(II) at cryptomelane/water interfaces. Chemosphere, 2018, 210, 392-400.	8.2	6
59	Biomembrane derived porous carbon film supported Au nanoparticles for highly reproducible surface-enhanced Raman scattering. New Journal of Chemistry, 2013, 37, 3131.	2.8	5
60	Decontamination performance of magnetic graphene oxide towards nickel ions and its underlying mechanism investigation by XAFS. Journal of Molecular Liquids, 2018, 258, 48-56.	4.9	4
61	Nitrogen Doped Nanoporous Carbon Derived from Zizania Latifolia for Adsorptive Removal of Bisphenol A. Journal of Nanoscience and Nanotechnology, 2019, 19, 1026-1034.	0.9	4
62	Facile Preparation of Activated Carbon from Peanut Shell for Determination of Bisphenol A in Human Urine by High-Performance Liquid Chromatography. Journal of Nanoscience and Nanotechnology, 2021, 21, 1439-1445.	0.9	4
63	One-Pot and Surfactant-Free Synthesis of Ultrafine PtSn Nanoparticles Supported on Onion-Like Nanocarbons Toward Efficient Methanol and Ethylene Glycol Oxidation Reactions. Journal of Nanoscience and Nanotechnology, 2020, 20, 2408-2415.	0.9	3

64 Back Cover Image, Volume 3, Number 6, November 2021. , 2021, 3, ii.